NASA TECHNICAL NOTE

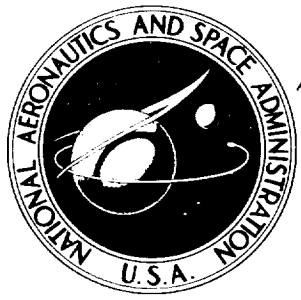

NASA TN D-1906

A THEORETICAL MODEL FOR SUNSPOT COOLNESS

by R. K. Jaggi
Goddard Space Flight Center
Greenbelt, Maryland

NATIONAL AERONAUTICS AND SPACE ADMINISTRATION • WASHINGTON, D. C. • OCTOBER 1963

National Aeronautics And Space Administration

ERRATA

NASA Technical Note D-1906

A THEORETICAL MODEL FOR SUNSPOT COOLNESS

R. K. Jaggi

October 1963

On pages 2, 3, and 4 replace H, H_m, and H_z with B, B_m, and B_z, respectively, in the text, equations and figure.

Issued 12-27-63

NASA-Langley, 1963

TECHNICAL NOTE D-1906

A THEORETICAL MODEL FOR SUNSPOT COOLNESS

By R. K. Jaggi

Goddard Space Flight Center
Greenbelt, Maryland

NATIONAL AERONAUTICS AND SPACE ADMINISTRATION

A THEORETICAL MODEL FOR SUNSPOT COOLNESS

(Manuscript Received July 1,1963)

by
R. K. Jaggi
Goddard Space Flight Center

SUMMARY

We have developed a theoretical model for the behavior of sunspots as individuals. Two models, called the current sheath model and the snowplow model, known in the theory of the pinch effect are worked out for the present problem of the sunspot expansion. Using the observational fact that the magnetic field of the sunspots grows to about 3,000 gauss in about ten days, numerical calculations based upon the current sheath model show that the sunspot area grows with the magnetic field and begins to pulsate when the magnetic field stops growing. The amplitude and frequency of oscillation depend upon the mass in the current sheath and the maximum magnetic field. The model suggests that the bright ring about the sunspots may exist at chromospheric height where the density of the material is about 10^9 particles/cm^3.

CONTENTS

A THEORETICAL MODEL FOR SUNSPOT COOLNESS

by
R. K. Jaggi
Goddard Space Flight Center

INTRODUCTION

Among the unsolved problems in solar physics reviewed by Goldberg and Dyer (Reference 1) is the difficulty in obtaining a theoretical interpretation of the mechanism of sunspot cooling. They proposed two possible explanations: The gas pressure in the sunspot is low because part of the total pressure is exerted by magnetic forces; in that case the configuration must approach an equilibrium in which the sum of the kinetic and magnetic pressures equals the kinetic pressure outside. The cooling could also be due to the forced expansion of a rising gas column. This second possibility is discarded because there is no observational evidence that the gas column is really rising. Many other models used to explain the coolness are based on the presence of a strong magnetic field (Reference 2, p. 172). Biermann (Reference 3) assumed that the low temperature is probably maintained by the strong magnetic fields inhibiting convective transport of energy, thus causing steep temperature gradients in the outer parts of the spots.

At this point it would be instructive to estimate the time in which the sunspot region, radiating like a blackbody, would fall from 6500 to 4500°K, the temperatures of the photosphere and a typical sunspot respectively. If convection is completely stopped, the time of this temperature fall is determined by

$$L \frac{\partial}{\partial t} (nkT) = \sigma T^4 ,$$

where $\sigma = 5.6 \times 10^{-5}$ erg/cm^2-sec-deg^4, and L, the total depth of the cool region, is given by

$$L \frac{nk(6500 - 4500)}{t} \approx \sigma(5000)^4 ,$$

with k the Boltzmann constant and σ the radiation constant. For $L = 10^8$ cm and $n = 10^{17}$, the above equation gives $t \approx 7.8$ sec, which shows that the region will cool down instantaneously. Some work has been done on the inhibition of convection in the presence of a magnetic field (References 4 and 5). The difficulty with Biermann's explanation is twofold: (1) it fails to explain the growth of the sunspot area with time; and (2) the cooling appears one or two days *after* the observation of the magnetic field. Also, any explanation of the sunspot coolness must at the same time explain the Evershed effect as well as the bright ring around the sunspots (as known by observation).

De Jager (Reference 2) has mentioned that the ions with energies greater than 3ev are reflected by the sunspot's magnetic field; but this is only effective in the upper, less dense part of the solar atmosphere and therefore does not explain lower temperature at the photospheric level. The particles reflected by the strong magnetic field of the sunspot will leave the region only if the mean free path is large enough to permit their escape. From Table 1 (in the last section of this paper), it is clear that the mean free path is large only in the upper chromosphere.

OBSERVATIONAL DATA

Before considering the theoretical model, we shall present some observational data. Most of this material was given in two articles by De Jager (Reference 2 and 6).

The development of sunspots forms part of the development of a *center of activity* (CA). De Jager (Reference 6) has divided the development of a CA into four parts: (1) pre-spot phase; (2) spot phase; (3) bipolar magnetic post-spot phase; and (4) unipolar magnetic phase. Of these, the second is of most interest in the present problem. A typical sunspot consists of an umbra and a penumbra, where the latter shows a radial filamentary structure, being slightly brighter than the former. The mean umbral area of large sunspots is of the order of 5×10^{-4} of the sun's visible hemisphere and the radius of the umbra is of the order of 2.2×10^{9} cm.

In the pre-spot phase the development of a bipolar magnetic field region as well as faculae are observable without the spots. The limits of the faculae coincide more or less with the sunspot region. The spot appears one or two days after the appearance of the magnetic field. The spot and the magnetic field region increase in area simultaneously.

A fifteen day time sequence of the development of a typical sunspot group is given by De Jager (Reference 2, p. 167). On the first day a single spot or a spot group without penumbra or without bipolar structure is observed on the sun. On the second day the bipolar group and penumbras of some of the bipolar spots appear. From five to ten days great bipolar spots as well as many small ones appear. From ten to fifteen days great bipolar spot groups remain without their smaller companions. During this time unipolar spots may also be observable.

Kiepenheuer (Reference 7) quotes Thiessen (Reference 8) as giving the following radial distribution of the vertical magnetic field in a sunspot:

$$H_z(r) \approx H_m\left(1 - \frac{r^2}{b^2}\right) , \tag{1}$$

where b is the radius of the outer edge of the penumbra, the subscript z denotes the z component of the field and the subscript m the field at the center of the spot, and r the radial distance measured from the axis of the spot. However, the magnetic field distribution as determined by Mattig (Reference 9) is of the form:

$$H_z(r) = H_m\left(1 - \frac{r^4}{b^4}\right) e^{-2r^2/b^2} .$$

Figure 1 is an approximate representation of this field (taken from Reference 2, p. 156). At the center of the spot the magnetic field H_m is of the order of a few thousand gauss. Assuming H_m to be 10^3 gauss we find that the magnetic pressure $H^2/8\pi$ is approximately 4×10^5 and is much higher than the kinetic pressure of the solar photospheric plasma $nkT \approx 3 \times 10^3$. Thus the sunspot is under the action of strong magnetic forces. Equating $H^2/8\pi$ with the kinetic pressure 3×10^3, we obtain $H \approx 260$ gauss. Therefore whenever the magnetic field is comparable to or higher than this value the sunspot will be under the action of strong magnetic forces.

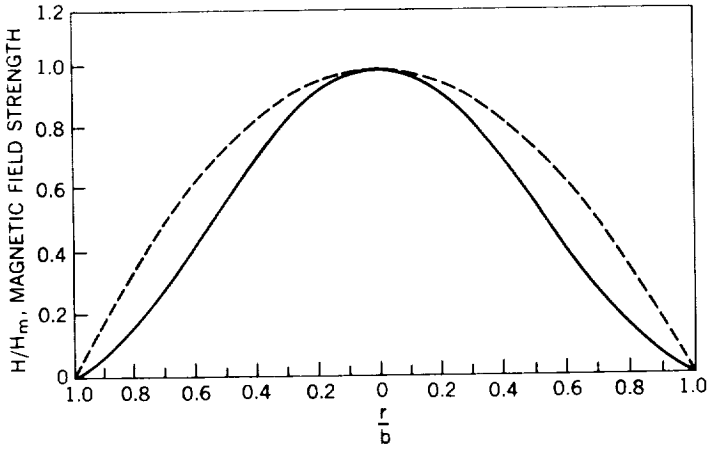

Figure 1–Variations of magnetic field strength over a sunspot as function of radius from the center of the spot. The distance to the spot center is expressed in terms of penumbral radius.

The time variation of the magnetic field observed over the sunspots is presented in Figure 2, which is taken from Cowling (Reference 10). Analytically the curve may be approximated by

$$H_m = 3000\left(1 - e^{-\frac{t}{2}}\right)\left(1 - e^{\frac{t}{5.5} - 10}\right) \qquad (2)$$

where t is measured in days.

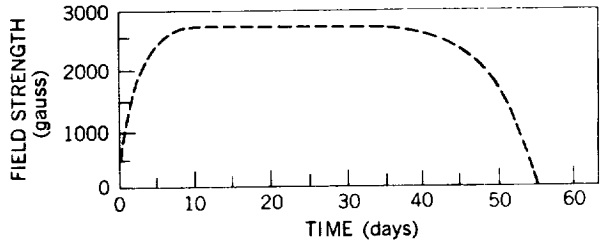

Figure 2–Variation of the field strength versus time in days for a 55-day spot.

We shall now discuss the adiabatic expansion of sunspots for the two models known as the current sheath and the snow plow models, in order to determine the rate of cooling in both instances.

THE CURRENT SHEATH MODEL

The basic equations of magnetohydrodynamics are

$$Nm_i \frac{d\mathbf{v}}{dt} = \frac{1}{c}\,\mathbf{j} \times \mathbf{B} - \text{grad } p \,, \qquad (3)$$

$$\frac{\partial N}{\partial t} = -\text{div}(N\mathbf{v}) \,,$$

$$\text{Curl } \mathbf{B} = \frac{4\pi}{c}\,\mathbf{j} \,, \qquad (4)$$

$$\text{div } \mathbf{B} = 0 ,$$

$$\frac{\partial \mathbf{B}}{\partial t} = \text{Curl } (\mathbf{v} \times \mathbf{B}) ,$$

$$\text{div } \mathbf{E} = 4\pi\epsilon ,$$

where the symbols have their usual meaning, ϵ is the charge density, and m_i the mass of an ion. From Equations 1 and 4, we obtain, in cylindrical coordinates

$$\mathbf{j} = \frac{cH_m}{4\pi} \left[0, \frac{2r}{b^2}, 0\right] ;$$

therefore the force,

$$\frac{1}{c} \mathbf{j} \times \mathbf{B} = \left[\frac{H_m r}{2\pi b^2}\left(1 - \frac{r^2}{b^2}\right), 0, 0\right] ,$$

is directed radially outward force. Consequently the cylinder must expand in the radial direction.

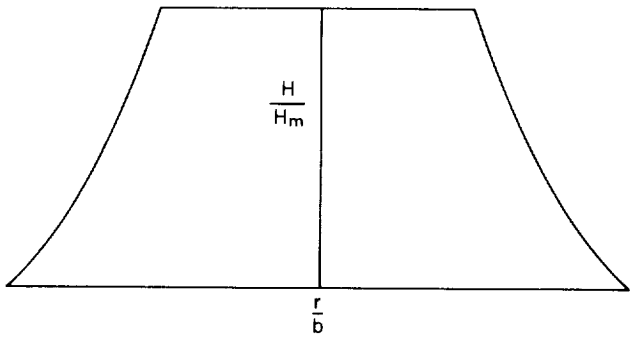

Figure 3–Modified form of Figure 1 used in calculating the expansion of sunspots.

To simplify the model we modify the distribution of the magnetic field given by Equation 1 in Figure 1 to that given in Figure 3. A portion of the cylinder is assumed to have a uniform magnetic field while the gradients of the magnetic field are assumed to be in the rest of the cylinder. The region occupied by this current is called "the current sheath." Equation (3) can be rewritten as

$$Nm_i \frac{d\mathbf{v}}{dt} = -\frac{1}{8\pi} \text{ grad } B^2 + \frac{1}{4\pi} (\mathbf{B} \cdot \nabla) \mathbf{B} - \text{grad } p .$$

In the present case the term $(\mathbf{B} \cdot \nabla) \mathbf{B} = 0$ because it is assumed that B is in the z-direction but there are no gradients in the z-direction. Integrating over the thickness of the current sheath, multiplying both sides by $2\pi r$, assuming that the acceleration over the cross-section of the current sheath and the density in the current sheath are uniform, we obtain

$$\frac{M}{\alpha} \frac{d^2 r}{dt^2} = 2\pi r \left(\frac{\bar{B}_i^2}{8\pi} + \bar{p}_i - p_0\right) , \tag{5}$$

where p_0 is the kinetic pressure due to the gases outside the cylinder, $\bar{p}_i$ the average kinetic pressure due to gases within the cylinder, and $\bar{B}_i$ the average magnetic field within the cylinder, and M the total mass contained in the cylinder. α has been introduced to insure that only a fraction of the total mass of the cylinder is contained in the current sheath. We shall assume that p_0 remains

constant and that $\bar{p}_i = p_0$ at $t = 0$. The changes in the kinetic pressure satisfy the ordinary adiabatic law

$$\frac{p}{N^{5/3}} = \text{Constant} \quad . \tag{6}$$

If B_0 is the initial magnetic field and r_0 the initial radius of the cylinder, the constancy of the magnetic flux in the cylinder gives

$$\pi r_0^2 B_0 = \pi r^2 \bar{B}_i \quad ,$$

or

$$\bar{B}_i = B_0 \left(\frac{r_0}{r}\right)^2 \quad . \tag{7}$$

Then, since N is proportional to $1/r^2$, Equation 6 yields

$$\bar{p}_i = p_0 \left(\frac{r_0}{r}\right)^{10/3} \quad . \tag{8}$$

Substituting Equations 7 and 8 into Equation 5 gives

$$\frac{M}{2\pi L} \frac{d^2 r}{dt^2} = r \left[\frac{B_0^2}{8\pi} \left(\frac{r_0}{r}\right)^4 + p_0 \left(\frac{r_0}{r}\right)^{\frac{10}{3}} - p_0 \right] .$$

Now by writing $r/r_0 = x$, $B_0^2/8\pi p_0 = \beta$ and $(m/2\pi a p_0)^{\frac{1}{2}} t' = t$ the above equation becomes

$$\frac{1}{x} \frac{d^2 x}{dt'^2} = \frac{\beta}{x^4} + \frac{1}{x^{\frac{10}{3}}} - 1 \quad . \tag{9}$$

To discuss the solution of Equation 9, the dependence of B on time must be known. According to observations, Equation (2), and Figure 2, the magnetic field rises in a matter of 10 days to a value of about 3000 gauss and remains at that value for about 40 days. Since the growth time is comparatively shorter than the lifetime of the magnetic field we may assume the magnetic field as a function of time given by Figure 4.

By assuming this magnetic field profile, it is possible to integrate Equation 9. The integration yields

$$\frac{1}{2} \dot{x}^2 = C - \frac{1}{2} x^2 - \frac{3}{4} x^{-\frac{4}{3}} - \frac{1}{2} \beta x^{-2}$$

If $t' = 0$, $x = 1$, $\dot{x} = 0$ can be assumed as the initial condition, then

$$\dot{x}^2 = \left(1 - x^2\right) + \frac{3}{2} \left(1 - x^{-\frac{4}{3}}\right) + \beta \left(1 - x^{-2}\right) \quad , \tag{10}$$

where the dot denotes differentiation with respect to t'. Figure 5 shows the relationship of $\dot{x}$ and x; and $x = 1$, $x = x^*$ are the solutions of

$$1 - x^2 + \frac{3}{2}\left(1 - x^{-\frac{4}{3}}\right) + \beta\left(1 - x^{-2}\right) = 0 .$$

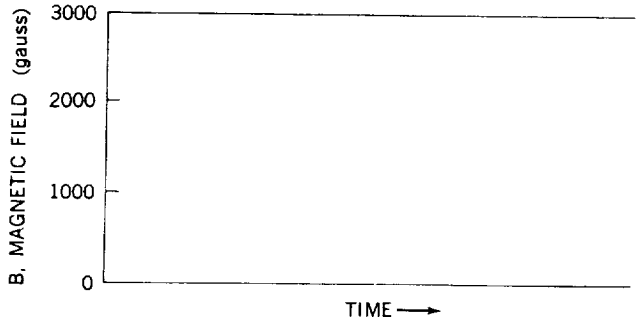

Figure 4—Profile used to deduce Equation 10.

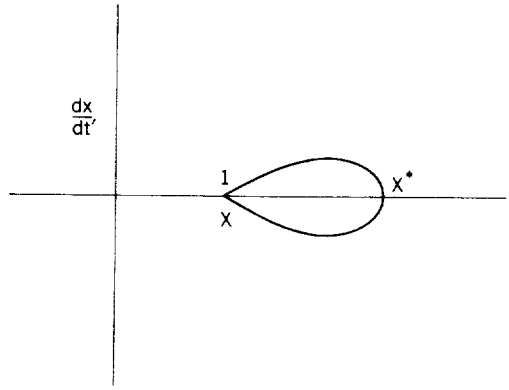

Figure 5—Representation of Equation 19.

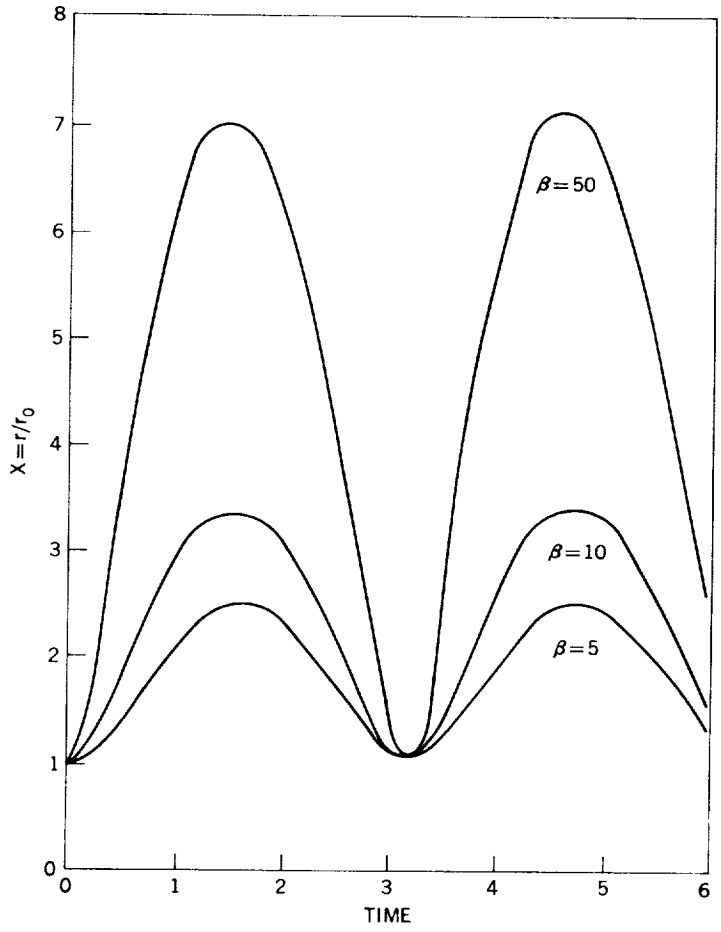

Figure 6—The solution of Equation 10 for β = 5, 10, 50.

Initially x is an increasing function of t because $\ddot{x} > 0$ at $t = 0$. Figure 5 shows that x is an oscillatory function of t. A complete solution of Equation 9, obtained on IBM 7090 computer, is represented in Figure 6 for β = 5, 10, 50. Here, the amplitude of oscillation increases with β.

To obtain a solution of Equation 9, in the general case, where the profile of the magnetic field is given by Equation 3 we must be cautious. If we use the expression for $\bar{B}_i$ given in Equation 3 the solution is unstable because $\ddot{x} > 0$ for all t and for any reasonable value of the magnetic field strength. For this reason we assume that the magnetic field is induced into the area at the rate given by Equation 3. The problem here is to find a magnetic field profile which gives $B_0(t)/x^2$ close to the curve given in Figure 2 and which gives a reasonably good fit for the area variation. Assuming then that

$$B_0(t) = B\left(1 - e^{-\frac{t}{2d}}\right)\left(1 - e^{\frac{t}{5.5d} - 10}\right),$$

where t is now measured in seconds and d is the number of seconds in one day, we have—instead of Equation 9

$$\frac{d^2x}{dt^2} = -x + x^{-\frac{7}{3}} + \frac{\zeta}{x^3}\left(1 - e^{-\frac{t}{2t_1}}\right)^2\left(1 - e^{+5.5\frac{t}{t_1} - 10}\right)^2, \tag{11}$$

where

$$t_1 = \frac{d}{\sqrt{\frac{M}{2\pi\alpha p_0}}}, \quad \zeta = \frac{B^2}{8\pi p_0}.$$

A solution of Equation 10 for $\zeta = 5$, $t_1 = 1$ is presented in Figure 7. The radius of the cylinder reaches a value of 1.6, oscillates about it and finally returns to its original value when the magnetic field has disappeared. The period of oscillation is 3 days and the amplitude of oscillation is about 0.25 r_0. Figures 8 and 9 present the velocity dx/dt and the temperature ratio T/T_0 as a function of t.

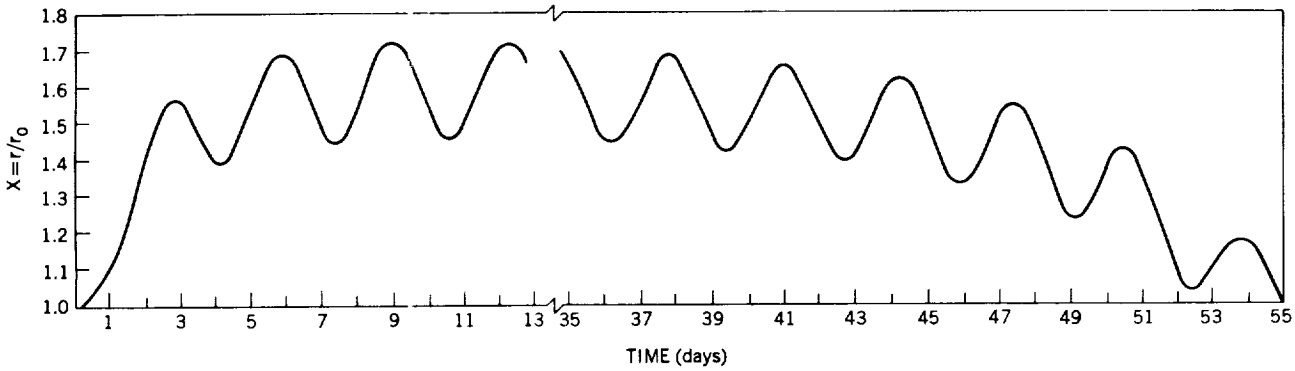

Figure 7--A 55-day spot represented by Equation 11 for $\zeta = 5$.

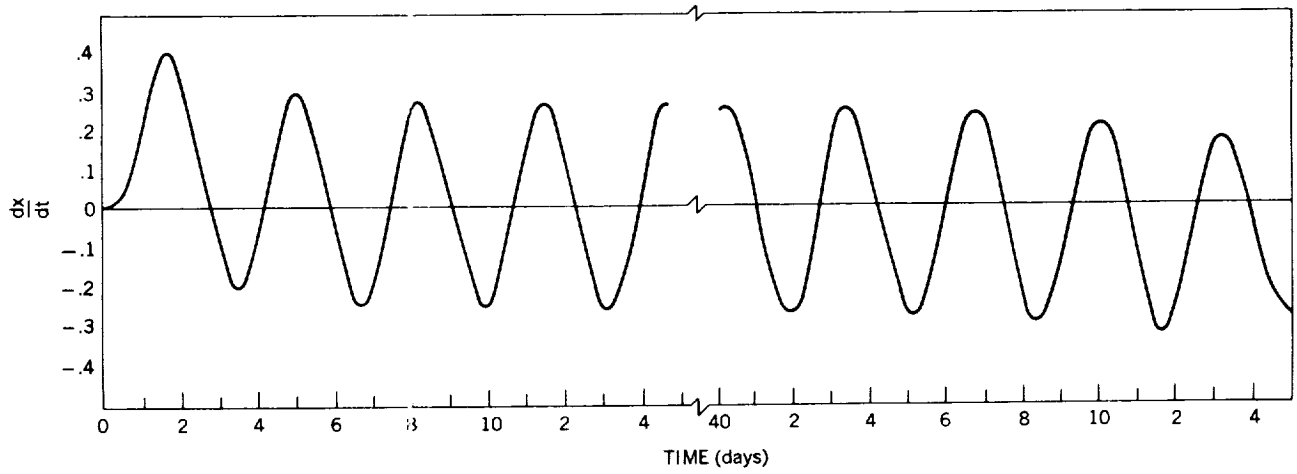

Figure 8—Representation of Equation 11 for $\zeta = 5$.

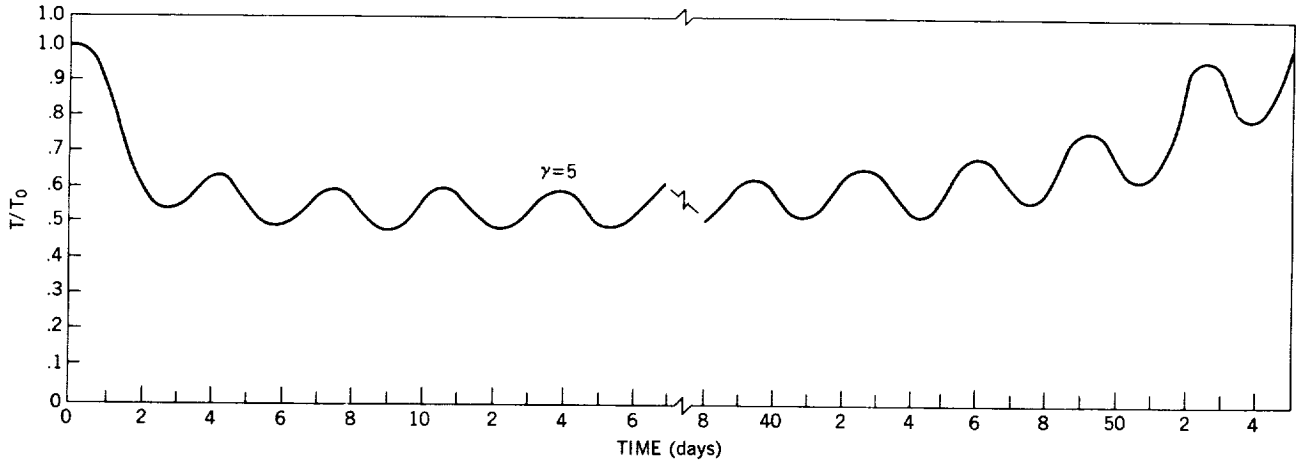

Figure 9–T/T_0 versus t represented by Equation 11 for $\zeta = 5$.

The assumption $t_1 = 1$ corresponds to $M/2\pi\alpha p_0 = (86,400)^2$ or $\alpha \approx 6 \times 10^3$ where we have used $r_0 = 10^9$ cm and $p = 10^4$. Therefore, a fraction $1/(6 \times 10^3)$ of the total mass of the cylinder is contained in the current sheath. For much higher values of α, the value of t_1 becomes large and the period of oscillation of the cylindrical sheath may become much smaller than that of Figure 7.

THE SNOW PLOW MODEL

In the snow plow model, first discussed by Rosenbluth (Reference 11), the magnetic field is homogeneous throughout the interior of the cylinder. The current sheath is in an infinitely thin layer of negligible mass. As the sheath expands it collects all the mass with which it comes in contact, as a snow plow collects the snow in its path. If r_0 is the initial radius of the cylinder and r the radius at any time t, the mass with the sheath is $\pi N m_i \left(r^2 - r_0^2\right)$ where N is the average number density of ions of mass m_i. Newton's equation of motion of the sheath then becomes

$$\frac{d}{dt}\left[\pi N m_i \left(r^2 - r_0^2\right) \frac{dr}{dt}\right] = 2\pi r \left(\frac{B_i^2}{8\pi} + \overline{p}_i - p_0\right) .$$

Using the transformations

$$\frac{r}{r_0} = x ,$$

$$\beta = \frac{B_0^2}{8\pi p_0} ,$$

$$\left[\frac{N m_i r_0^2}{2p_0}\right]^{\frac{1}{2}} t' = t ,$$

we obtain the equation

$$\frac{d}{dt'}\left[(x^2 - 1)\frac{dx}{dt'}\right] = x\left(\frac{\beta}{x^4} + x^{-\frac{10}{3}} - 1\right), \tag{12}$$

where Equations 7 and 8 were used to express B_i in terms of B_0 and $\bar{p}_i$ in terms of p_0. With the magnetic field profile of Figure 4, this equation was solved on an IBM 7090 and its solution is shown graphically in Figure 10. The initial conditions satisfied by this equation are $t' = 0$, $x = 1$, $\dot{x} = \sqrt{3/2}$. The solution is shown in Figure 10 for β = 5, 10, and 50.

A peculiar feature of this differential equation is that while in the expanding phase the sheath collects all mass with which it comes in contact; however, in the contracting phase it is losing its mass–not exactly in the same way as a snow plow because the snow plow loses its mass instantaneously when the direction of the velocity is reversed. We can therefore only follow the calculation of the snow plow model until the velocity reverses in sign. For that reason this model will not be discussed in detail.

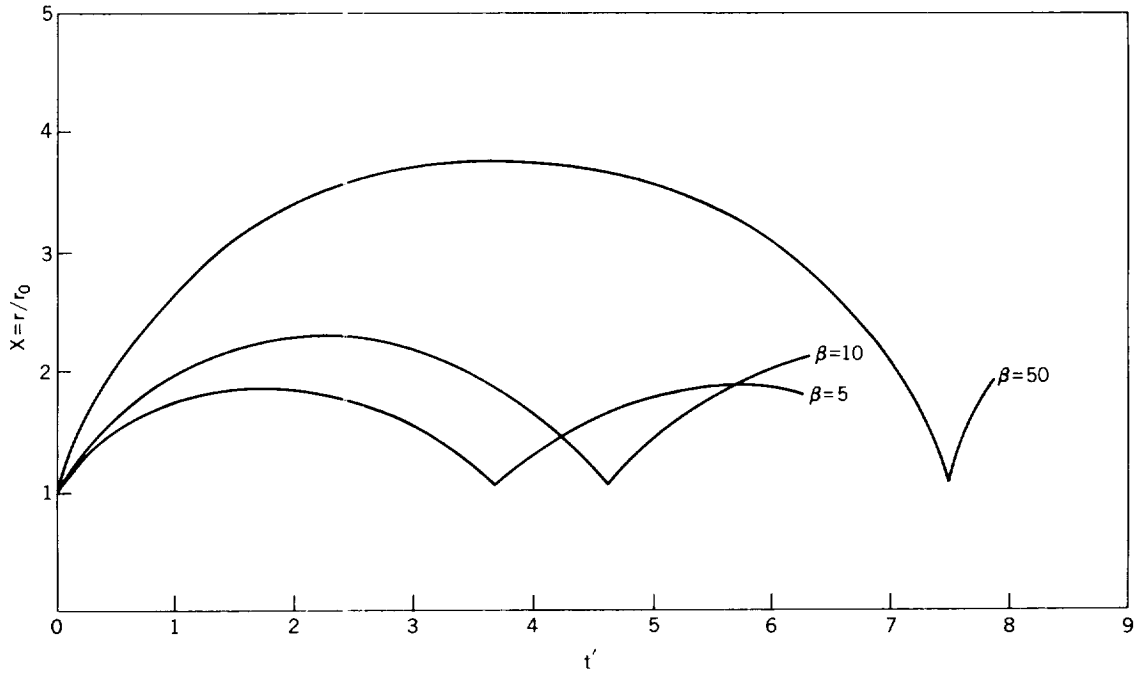

Figure 10–The solution of Equation 12 for β = 5, 10, 50.

THE EFFECT OF DENSITY AND PRESSURE GRADIENTS ON THE DYNAMICS OF SUNSPOTS

The pressure and density both rise in the lower levels of the photosphere. Figures 11 and 12 show the graph of the variation of the density P and the pressure p from the surface of the photosphere to the depth of a few hundred kilometers. In the solar photosphere, the pressure rises more

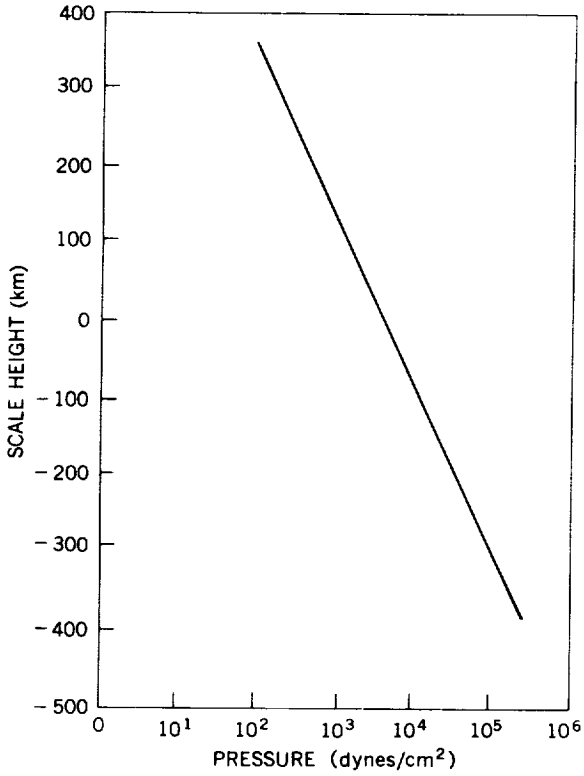

Figure 11–Variation of p versus height in the solar photosphere (Taken from Reference 10, p. 127, Table II).

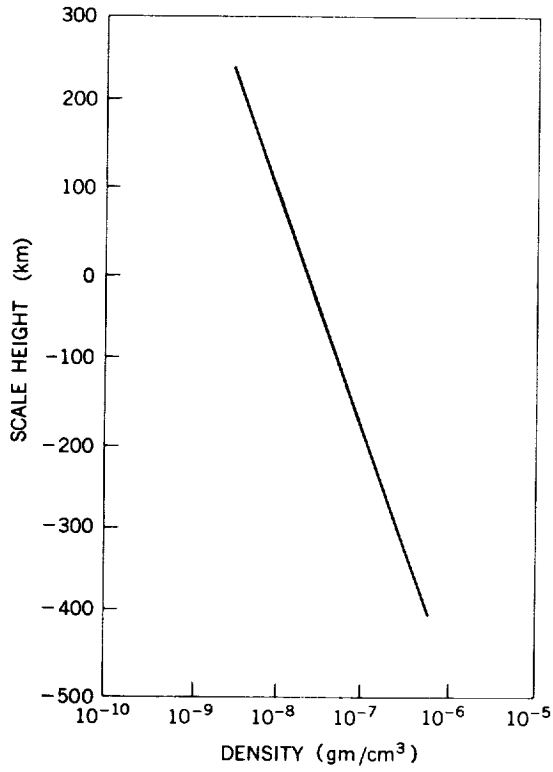

Figure 12–Variation of ρ versus height in the solar photosphere (Taken from Reference 10, p. 127, Table II).

rapidly with depth than the density. For example at a depth of about 400 km the pressure is about 20 times that at the surface of the photosphere and the density is about 10 times that at the surface. If the photosphere is assumed to be stratified, the lower layers have less amplitude of oscillation than those at the surface. Also if the lower layers oscillate independently the frequency of oscillation can be different at the lower levels. Replacing p_0 with $20p_0$ in Equations 5 and 8, we obtain in place of Equation 9:

$$\frac{1}{x}\frac{d^2x}{dt'^2} = \frac{\beta}{x^4} + \frac{20}{\frac{10}{x^3}} - 20 . \qquad (13)$$

The solution of this equation is shown in Figure 13.

The frequency of oscillation of x in Figure 13 is about .75, and in Figure 6 it is about 3.2. Thus

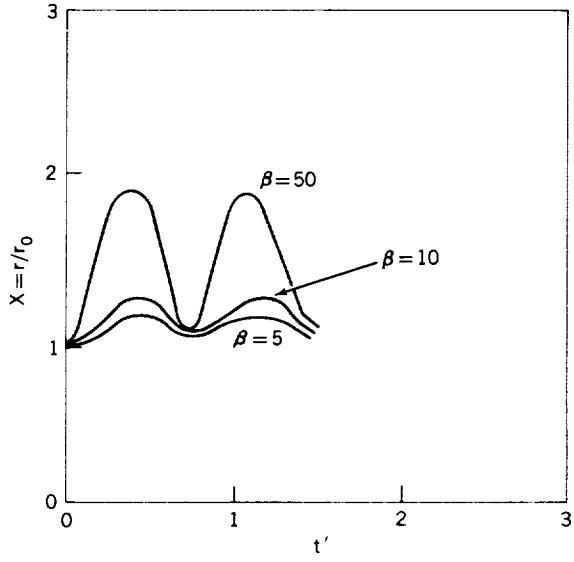

Figure 13–Representation of Equation 13 for β = 5, 10, 50.

the two periods of oscillation are

$$t_1 = 3.2\left(\frac{\pi r_0^2 \rho'}{2\pi a p_0}\right),$$

$$t_2 = 0.3\left(\frac{\pi r_0^2 \rho}{2\pi a p_0}\right).$$

Therefore the ratio $.75/3.2 = (\rho'/\rho)^{\frac{1}{2}}$ is greater than or less than one depending on whether $\rho' \gtrless 18.2\rho$.

In order to draw any conclusions about the frequency of oscillation we must know the variation of density with depth. From the figures given by Minneart (1953), in Figure 12, we find that $\rho' \simeq 10\,\rho$. We therefore conclude that the period of oscillation at lower levels in the solar photosphere is approximately the same as at the surface. This subject will be taken up in a later paper.

THE BRIGHT RING AROUND SUNSPOTS

During the initial growth of the 55-day spot considered the velocity of the current sheath has a value of about 1-10 km/sec. Charged particles with their thermal velocities suffer reflection from these initially outward moving sheath and gain energy. These particles will then move a few mean free paths before loosing the energy gained from reflection. Therefore additional light in the solar photosphere or chromosphere, will be generated and a bright ring around a spot, with a width of the order of a mean free path will be created.

The self collision time of particles of mass m and charge e is given by

$$t_c = \frac{m^{\frac{1}{2}}(3kT)^{\frac{3}{2}}}{8 \times 0.714\pi e^4 z^4 \log \Lambda},$$

where

$$\Lambda = \frac{3}{2e^2 z^2}\left(\frac{k^3 T^3}{\pi n}\right)^{\frac{1}{2}}.$$

Thus the mean free path is

$$L = \sqrt{\frac{3kT}{m}}\, t_c$$

$$= \frac{(3kT)^2}{8 \times 0.714\pi e^4 z^4 \log \Lambda}$$

$$\approx \frac{1.8 \times 10^5 T^2}{N \log \Lambda},$$

and is independent of the mass of the particle. In Table 1 this quantity is given for $N = 10^6$ to

Table 1

Mean Free Path of a Charged Particle for the Temperatures and Number Densities Shown.

Temperature (°K)	Mean Free Path of Charged Particles			
	$N = 10^6 \frac{\text{particles}}{\text{cm}^3}$	$N = 10^9 \frac{\text{particles}}{\text{cm}^3}$	$N = 10^{12} \frac{\text{particles}}{\text{cm}^3}$	$N = 10^{15} \frac{\text{particles}}{\text{cm}^3}$
10^3	1.4×10^4	19		
10^4	1.1×10^5	1.4×10^3	1.9	
10^5	$.91 \times 10^8$	1.1×10^5	1.4×10^2	.19
10^6	$.79 \times 10^{10}$	$.93 \times 10^7$	1.1×10^4	14.5

10^{15} particles/cm^3 and T = 10^3 to 10^6 °K. From this table it appears that the upper chromosphere is the region where the mean free path is measurable by optical methods. Near the photosphere the mean free path is too short and the thickness of the bright ring will probably be too small to be measured.

A radially outward moving current sheath moving with a velocity of the order of one km/sec produces a shock wave the thickness of which is of the order of

$$10 \frac{c}{\omega_p} = 10 \frac{3 \times 10^{10} \left(10^{-27}\right)^{\frac{1}{2}}}{\left(4 \times 10^{15} \times 25 \times 10^{-20}\right)^{\frac{1}{2}}}$$

$$\approx \frac{1}{10} \text{ cm}$$

(Reference 13) which is also too small. Table 2 shows the variation of c/ω_p with density.

Table 2

Variation of c/ω_p with Number Density.

N $\left(\frac{\text{Particles}}{\text{cm}^3}\right)$	c/ω_p
10^3	1.7×10^4
10^6	540
10^9	17
10^{12}	.54
10^{15}	1.7×10^{-2}

It is only in the upper chromosphere that the thickness of the shock is sufficient to be observable. Therefore, according to the present analysis, the bright ring should be observed to be expanding.

ACKNOWLEDGMENTS

The author would like to thank Drs. W. N. Hess, J. M. Burgers, and D. A. Tidman for fruitful discussions and Mr. J. Grunwald, and Mrs. E. Glover for help with programming the equations for the computer.

REFERENCES

1. Goldberg, L. and Dyer, E. R., Jr., "The Sun," *In:* "Science and Space," (L. V. Berkner and H. Odishaw, eds.): 307-340, New York: McGraw-Hill, 1961.
2. deJager, C., "Structure and Dynamics of the Solar Atmosphere," *In:* "Handbuch der Physik," v. 52 (S. Flugge, ed.): 80-362, Berlin: Springer-Verlag, 1959.
3. Biermann, L., "Der Gegenwärtige Stand der Theorie Konvektiver Sonnenmodell," *Vierteljahrsschrift Astron. Ges.* 76(4):194-200, 1941.
4. Thompson, W. B., "Thermal Convection in a Magnetic Field," *Phil. Mag.* Ser. 7, 42:1417, 1951.
5. Chandrasekhar, S., "On the Inhibition of Convection in a Magnetic Field," *Phil. Mag.* Ser 7, 43:501, 1952.
6. deJager, C., "The Development of a Solar Centre of Activity," *In:* "Vistas in Astronomy," vol. 4 (A. Beer, ed.): 143-183, Oxford, New York, Pergamon Press, 1961.
7. Kiepenheuer, K. O., "Solar Activity," *In:* "The Sun," (G. P. Kuiper, ed.): 322-465, Chicago: University of Chicago Press, 1953.
8. Thiessen, G., "The Magnetic Field Strength in Sunspots," *Naturwissenschaften* 40(7):218-219, 1953.
9. Mattig, W., "Die Radiale Verteilung der Magnetischen Feldstaerke in Normalen Sonnenflocken," *Zeits. Astrophysik* 44(4):280-300, 1958.
10. Cowling, T. G., "The Growth and Decay of the Sunspot Magnetic Field," *Mon. Not. Roy. Astron. Soc.* 106(3):218-224, 1946.
11. Rosenbluth, M., Garwin, R., and Rosenbluth, A., "Infinite Conductivity Theory of the Pinch," Los Alamos Scientific Lab., New Mexico Rept. No. LA 1850, September 14, 1954 (Declassified 1958).
12. Minneart, M., "The Photosphere," *In:* "The Sun," (G. P. Kuiper, ed.): 88-185, Chicago: University of Chicago Press, 1953.
13. Adlom, J. A. and Allen, J. E., "The Structure of Strong Collision Free Hydromagnetic Waves," *Phil. Mag.* 3:448, 1958.